

University of Arkansas, Fayetteville  
**ScholarWorks@UARK**

---

Biological Sciences Undergraduate Honors Theses

Biological Sciences

---

5-2015

# Fluorescent cell imaging studies of antitumor natural macrocycle ipomoeassin F

Margaret Grace Oliver

*University of Arkansas, Fayetteville*

Follow this and additional works at: <http://scholarworks.uark.edu/biscuht>

---

## Recommended Citation

Oliver, Margaret Grace, "Fluorescent cell imaging studies of antitumor natural macrocycle ipomoeassin F" (2015). *Biological Sciences Undergraduate Honors Theses*. 8.  
<http://scholarworks.uark.edu/biscuht/8>

This Thesis is brought to you for free and open access by the Biological Sciences at ScholarWorks@UARK. It has been accepted for inclusion in Biological Sciences Undergraduate Honors Theses by an authorized administrator of ScholarWorks@UARK. For more information, please contact [scholar@uark.edu](mailto:scholar@uark.edu).

**Fluorescent Cell Imaging Studies of Antitumor Natural Macrocycle Ipomoeassin F**

An Honors Thesis submitted in partial fulfillment of the  
requirements of Honors Studies in Biology

By Margaret Grace Oliver

Spring 2015

Biology

J. William Fulbright College of Arts and Sciences, the University of Arkansas

## **Acknowledgements**

This research project could not have been completed without the help of many individuals. I want to especially thank Dr. Wei Shi for being fundamental to my development as a scientist and an academic, and for all of his guidance in my project's many twists and turns throughout its development. I would also like to thank Drs. Guanghui Zong, Mugunthan Govindarajan, and Hazim Al-Jewari for their frequent assistance in my endeavors, and for the materials and data that they contributed to my project. Also fundamental to this project is the University of Arkansas Honors College, which enables and encourages students to undergo the valuable learning experience that is undergraduate research. Finally, I would like to thank the Arkansas Department of Higher Education and the University of Arkansas for their joint support via the Statewide Undergraduate Research Fellowship that I received for the spring and fall semesters of 2014. This grant allowed me to complete my research as it was meant to be completed, without worry of financial limitations.

## **Table of Contents**

Acknowledgments ...	2
Abstract ...	4
Introduction ...	5
Results ...	9
Conclusions ...	24
Experimental Materials and Methods ...	28
References ...	38
Appendices ...	39

## Abstract

Ipomoeassin F is one member of a family of macromolecules isolated from the leaves of the morning glory flower, *ipomoea squamosa*, which has been used as a homeopathic cancer remedy for centuries (Zhu, Huang, Zheng, Zhu, & Yang, 2013). It has been proven to be highly cytotoxic to many cancer cell lines, but nothing is yet known of its mode of action in the cell (Cao, et al., 2007). To begin progress towards understanding the mode of action of ipomeoassin F, this study aimed to perform fluorescence imaging studies for the ultimate purpose of determining its cellular localization in MDA-MB-231 breast cancer cells. Attempts were made at both direct and indirect fluorescence imaging.

To perform direct fluorescence imaging studies, two fluorescent dye probes known for their stability and ease of modification were synthesized: BODIPY and coumarin. The BODIPY synthesis was very challenging, and yield was very poor, averaging 0.46% yield. Both were subjected to SAR studies to evaluate their suitability for use in fluorescence imaging. Cytotoxicity assays revealed that neither dye probe can be used to study ipomoeassin F via direct fluorescence, because their addition to the ipomoeassin F molecule too severely inhibits its normal cytotoxic activity.

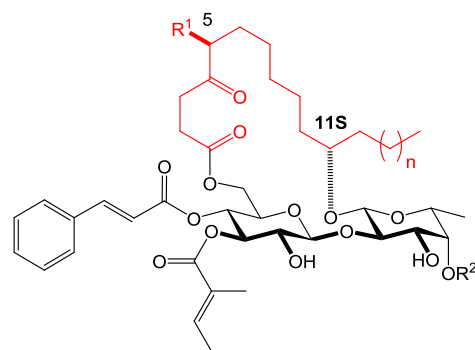
To perform indirect fluorescence imaging studies, click chemistry was performed between a triazole coumarin fluorophore and a biorthogonal alkyne analog of ipomoeassin F to yield a fluorescent product. The reactions performed as part of this project were preliminary, and included a calibration titration, two model system reactions, and a study of the analog. These reactions elucidated conditions and suggestions that will be useful in future studies of ipomoeassin F.

## Introduction

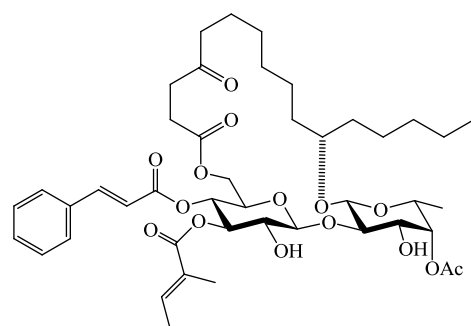
Cancer remains one of the leading causes of death for adults in the United States. This disease touches everyone in this country, but cures for most types of cancer have remained elusive. For many diseases including cancer, researchers have always looked to nature for inspiration and materials to test for treatment. Between 1981 and 2010, 68% of new FDA-approved anticancer medications and 60% of new antitumor medications were derived from or inspired by natural products (Newman & Cragg, 2012). The term “natural products” simply describes some molecules that occur naturally in a living organism. Oftentimes these naturally-derived pharmaceuticals are more effective at killing cancerous cells compared to other synthetically-derived chemotherapeutic agents, and so they are of great interest.

The largest obstacle in developing a drug from a natural product is the initial lack of knowledge about its exact mode of action in cells, which is essential to optimizing the natural product for therapeutic and preventative applications. This role can begin to be understood by first identifying the natural product’s target proteins that it acts upon, which then implicate related processes and rule others out. For example, if imaging studies indicate that a natural product only localizes in the membrane of cancer cells prior to killing them, then many other pathways to cell death that do not involve the cellular membrane can be ruled out as the targets of the natural product treatment. The purpose of this research project is to investigate the localization of a specific macrocycle that has recently been isolated from the leaves of *Ipomoea squamosa* and found to be potentially cytotoxic to cancer cells.

Ipomoeassin F (Figure 1) is a macrocycle—a cyclic molecule with a ring structure of 12 or more atoms—that was isolated in 2007 from the leaves of *Ipomoea squamosa*, commonly known as the morning glory, which is native to South America (Cao, et al., 2007). It is one of the six ipomoeassins, which are derivatives of this flower that has been used as a homeopathic cancer treatment in China for centuries (Zhu, Huang, Zheng, Zhu, & Yang, 2013). Ipomoeassins A, B, C, D, and E were isolated two years earlier, and in 2007 ipomoeassin F was isolated in very



General structure of ipomoeassins A-F



ipomoeassin F

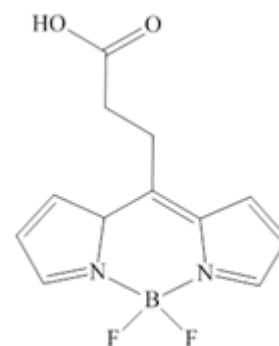
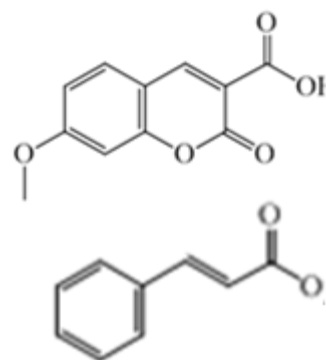
**Figure 1: ipomoeassin structures**

small amounts (Cao, et al., 2007). Initial studies have found that the ipomoeassins have variable cytotoxicity against cancer cells, and that ipomoeassin F is the most potent of the family (see Table 1). Ipomoeassin F’s cytotoxicity has been found to be as effective as or more effective than many types of anticancer medications currently in use, such as Paclitaxel—also known as Taxol. The  $IC_{50}$  values of course can vary greatly depending on the cancer cell lines that are tested, which fits into the current belief in the field that there can never be a “one-size-fits-all” cure for all types of cancer (see Table 1, Cao, et al., 2007). A postdoctoral fellow obtained ipomoeassin F for study via a newly-developed chemical synthetic pathway.

**Table 1: Selected Cytotoxicity Data for Ipomoeassins**

Ipomoeassin	IC <sub>50</sub> (nM)			
	L-929	U937	HT-29	MDA-MB-231
A	77.8	202	46.1	42.6
B		134	396	2700
C	>1000			
D	135	7.9	11.8	19.9
E	>1000	163	393	1633
F	7.4	2.6	4.2	9.4

In pursuit of understanding the cellular localization of ipomoeassin F, this study utilizes techniques of fluorescent cell imaging. This is an alternative to radioactive isotope-labeling techniques, which are expensive and hazardous to work with (Giessler, Griesser, Gohringer, Sabirov, & Richert, 2010). For the experiments, two fluorescent dye probes were synthesized: BODIPY (Figure 2) and coumarin (Figure 3). BODIPY, or boradiazaindecene, was selected to be used first because it has many favorable properties as a fluorescent dye for potential use in *in vivo* study. It has excellent fluorescence, in that the brightness of its fluorescent signal is strong compared to “background noise” from naturally fluorescent cellular components, and can easily be detected. BODIPY is also very stable in many pH environments, levels of exposure to light, and solvents (Ulrich, Ziessel, & Harriman, 2007). Coumarin was synthesized by a post-doctoral fellow for potential use in

**Figure 2: BODIPY****Figure 3: Coumarin (above) and the cinnamate moiety**



addition to BODIPY, and it was selected because it is structurally similar to the cinnamate moiety in ipomoeassin F (see Figure 3). The key structural features in coumarin are the preservation of the benzene ring and the double bonds that are found in the original cinnamate moiety (see Figure 3).

In order to utilize the fluorescent dye probes in a fluorescent cell imaging study, they must be attached to ipomoeassin F to form an analog. However, not all potential positions to add the dye probe are equal. Because some functional groups are more necessary for the biological activity than others, if certain key functional groups are altered in order to add the dye probe, the bioactivity of the derived probe may be compromised. To evaluate which functional groups are necessary for function, structure activity relationship (SAR) studies need to be performed. However, these studies have not yet been published for ipomoeassin F, so it could not be determined in advance which modifications would result in a loss of activity. Therefore, cytotoxicity assays were performed on the original ipomoeassin F molecule and all dye-tagged analogs—or their structural equivalent, in the case of BODIPY—cultured with MDA-MB-231 human breast cancer cells to ascertain any negative effects on cytotoxicity.

As a protective measure in case the BODIPY and coumarin moieties damaged the cytotoxic activity of ipomoeassin F, an alternative indirect method of fluorescent cell imaging was explored by using click chemistry. Indirect fluorescence imaging is basically the combination of two molecules—where at least one is not fluorescent—whose product is fluorescent (see Figure 4). In this study, the combination will be done



**Figure 4: A Simple Representation of Indirect Fluorescence Imaging**

via click chemistry; in nature, this can occur through covalent attachments. The term “click chemistry” describes a chemical reaction that is high yielding, simple to perform, produces only easy-to-remove byproducts, and can be performed in simple solutions (Kolb, Finn, & Sharpless, 2001). Click chemistry was used in these experiments to combine two non-fluorescent molecules together to produce a fluorescent product—this is called fluorogenic click chemistry—, an analog of ipomoeassin F that will be cultured with MDA-MB-231 cells to perform fluorescent cell imaging. The major downside to this as opposed to working with BODIPY or coumarin-labeled ipomoeassin F is that the click chemistry reaction cannot be conducted in living cells. The benefit is that the initial modification to the ipomoeassin F molecule is much smaller compared to the modification of adding BODIPY or coumarin, so the click chemistry reaction is more likely to preserve the normal biological activity of ipomoeassin F.

## **Results**

### **BODIPY Synthesis**

Multiple attempts were made at the BODIPY synthesis. The first attempt was a replication of the literature protocol, to scale. The second attempt began with a 10x increase in scale of the first step, and the products from that first step were used to complete the second and third attempts at the complete synthetic pathway.

**Table 2: BODIPY Synthesis Percent Yield by Attempt and Step**

	Step 1 Yield	Step 2 Yield	Step 3 Yield	Total Yield
Attempt 1	67.00%	1.20%	37.21%	0.10%
Attempt 2	66.45%	6.32%		
Attempt 3		8.55%	14.39%	0.82%
Average	66.72%	5.36%	25.79%	0.46%

Some cells in Table 1 are grayed out because no data were collected for that particular step. There are no data for attempt 3 step 1 because attempt 2 step 1 was performed at a large scale, so leftover product from attempt 2 step 1 was used to perform the rest of attempt 3. The yield for attempt 2 step 1 was used in the calculations for total percentage yield for attempt 3. The total percentage yield could not be calculated for attempt 2 because it was not completed, due to very poor yield for attempt 2 step 2.

The synthetic yield was consistent and quite high for step 1, which was by far the simplest step to perform. It is very clear in the percentage yield data that the greatest threat to overall synthetic yield was the second step. The difficulty of isolating the product via silica chromatography was certainly a major factor in the poor yield for all attempts of step 2. The yield for step 3 was an improvement, though it was still significantly lower than the average for step 1.

$^1\text{H}$  NMR was performed in deuterated chloroform for the final product from each of the three attempts. A  $^{13}\text{C}$  NMR was performed only for the final product of the final attempt. Consistently, the spectra reveal noteworthy impurities in the products (see Appendix A for NMR spectra from each synthetic attempt). Ideally, the pure product should have  $^1\text{H}$  NMR peaks at 2.45 (s, 6H), 2.52 (s, 6H), 2.64-2.69 (m, 2H), 3.31-3.35

(m, 2H), and 6.08 (s, 2H) ppm (Machida, Tsubamoto, Kato, Harada, & Ohkanda, 2013). Examining the proximity of the three  $^1\text{H}$  NMR spectra to this information, it appears that the final product from Attempt 2 was the most pure (see Figure 15 in Appendix A). This is largely because it does not have so many extraneous “contamination” peaks as the spectra for Attempt 1 (see Figure 14 in Appendix A), and the intensity of the signal is much higher than in Attempt 3 (see Figure 16 in Appendix A).

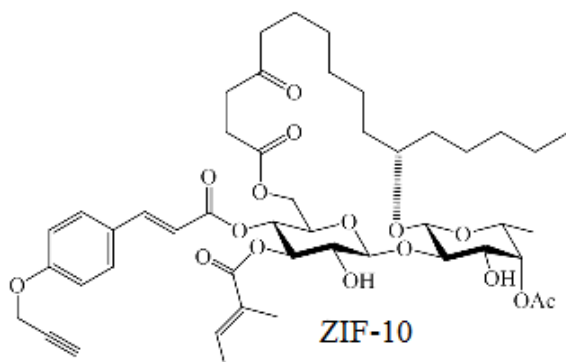
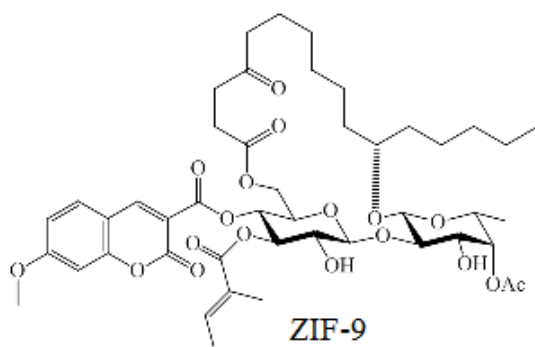
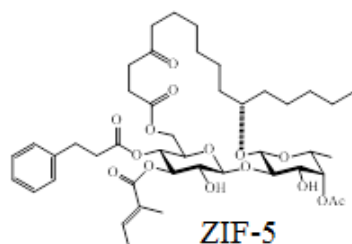
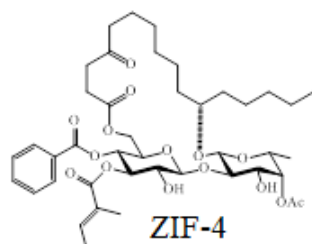
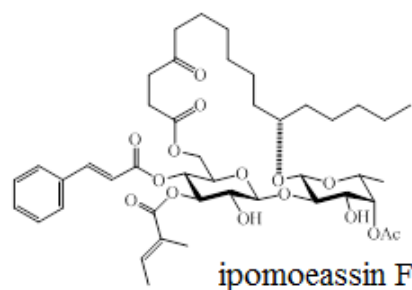
### **Cytotoxicity Assays**

The cytotoxicity assays were performed using a plate reader and the Gen5 software program. The fluorescence readings were imported into GraphPad, another software program, which calculated the cytotoxicity curves and the  $\text{IC}_{50}$  values. Another measure,  $\text{IC}_{50}$  index, was calculated as a ratio of the  $\text{IC}_{50}$  of the ZIF compounds to the  $\text{IC}_{50}$  value for unmodified ipomoeassin F, to serve as a simple numerical representation of how much more or less effective the ZIF compounds are. For example, a compound with an  $\text{IC}_{50}$  index of 1000 compared to ipomoeassin F would be 1000 times less effective, but a compound with an  $\text{IC}_{50}$  index of 0.001 would be 1000 times more effective. Taxol served as a positive control. The  $\text{IC}_{50}$  values for Taxol listed in Table 2 are those obtained via the same cytotoxicity assay trials, to ensure that the technique was consistent.

**Table 3: IC<sub>50</sub> Values for MDA-MB-231**

<b>Treatment Type</b>	Taxol	Ipomoeassin F	ZIF-4	ZIF-5	ZIF-9	ZIF-10
<b>IC<sub>50</sub> (NM)</b>	11.2	6.44	760.0 (IC <sub>50</sub> index 119)	947.5 (IC <sub>50</sub> index 148)	9329 (IC <sub>50</sub> index 1448.6)	9.69 (IC <sub>50</sub> index 1.5)

The cytotoxicity data here for Taxol, ZIF-4, and ZIF-5 (see Figure 5) were provided by Dr. Hazim Al-Jewari, a post-doctoral fellow in the lab. His data were also used to verify the accuracy of the cytotoxicity values obtained in this study for ipomoeassin F, ZIF-9, and ZIF-10 (see Figure 5), which are shown in the table above.



As seen in the table, ipomoeassin F can kill 50% of cultured cells at a significantly lower concentration than Taxol, a real-world oncological treatment. It is because of this property that this compound is of such interest to the Shi Group. The remaining cytotoxicity values serve to illustrate the utility of various analogs of ipomoeassin F, particularly in the potential for using BODIPY, coumarin, and ZIF-10 in fluorescent imaging studies. ZIF-4 and ZIF-5 are both analogous to the structure of a BODIPY-tagged ipomoeassin F fluorescent probe, so the fact that their cytotoxicity values are much higher than unmodified ipomoeassin F suggests that the addition of BODIPY to ipomoeassin F without the conjugated double bond would significantly impact its normal

**Figure 5: Ipomoeassin F analogs of interest**

intracellular function as an antitumor agent. ZIF-9 already contains the coumarin moiety—it is not merely analogous to a coumarin-tagged ipomoeassin F molecule. Its cytotoxicity is, as seen in the  $IC_{50}$  index value in particular, is over 1,000 times weaker than that of unmodified ipomoeassin F, and so it is quite unsuitable for meaningful investigation of ipomoeassin F's cellular localization. However, ZIF-10, the biorthogonal alkyne analog of ipomoeassin F, is quite similar to that of unmodified ipomoeassin F, which is why it was ultimately chosen for future study via indirect fluorescence imaging. Dr. Hazim Al-Jewari has collected a range of cytotoxicity values for ZIF-10 in MDA-MB-231 cells—some with an  $IC_{50}$  index as low as 0.8, meaning that the ZIF-10 in that trial was even more potent than unmodified ipomoeassin F.

#### ZIF-4, ZIF-5, ZIF-9, ZIF-10, Ipm-F, & Taxol, MDA-MB-231

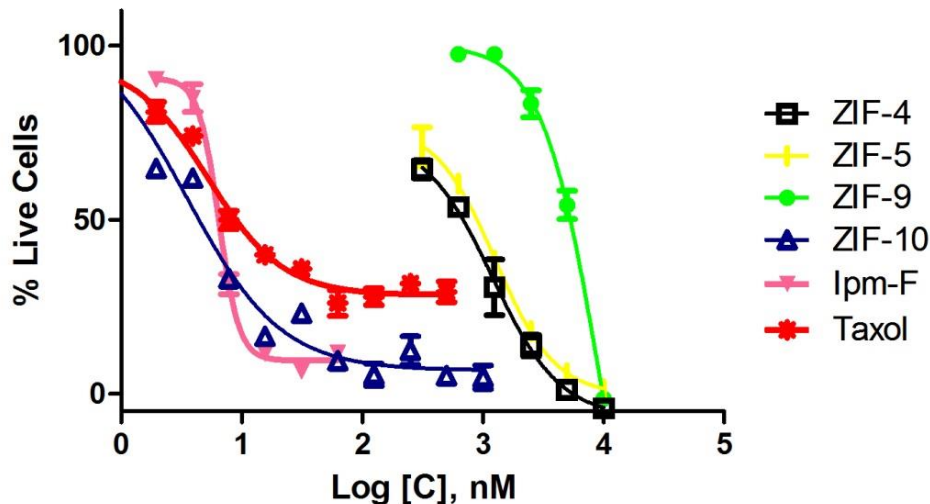


**Figure 6: Cytotoxicity Curves for MDA-MB-231**

The above graph was provided by Dr. Hazim Al-Jewari. It primarily serves to highlight the similarity in cytotoxicity trends between ZIF-10 and unmodified ipomoeassin F (the blue and pink lines, respectively). It also highlights both ZIF-10 and

ipomoeassin F's potency compared to Taxol. This graph further demonstrates that ZIF-4, ZIF-5, and ZIF-9 are substantially less potent than ipomoeassin F at all concentrations, requiring several points more on a logarithmic scale of concentration than ipomoeassin F, taxol, and ZIF-10 to reach their IC<sub>50</sub> value. Because none of the dye-tagged analogs—ZIF-9—or their structural equivalents—ZIF-4 and ZIF-5—were suitable for direct fluorescence imaging due to their poor cytotoxicity, indirect fluorescence imaging via click chemistry was explored utilizing the much more promising ZIF-10.

### Click Chemistry Reactions

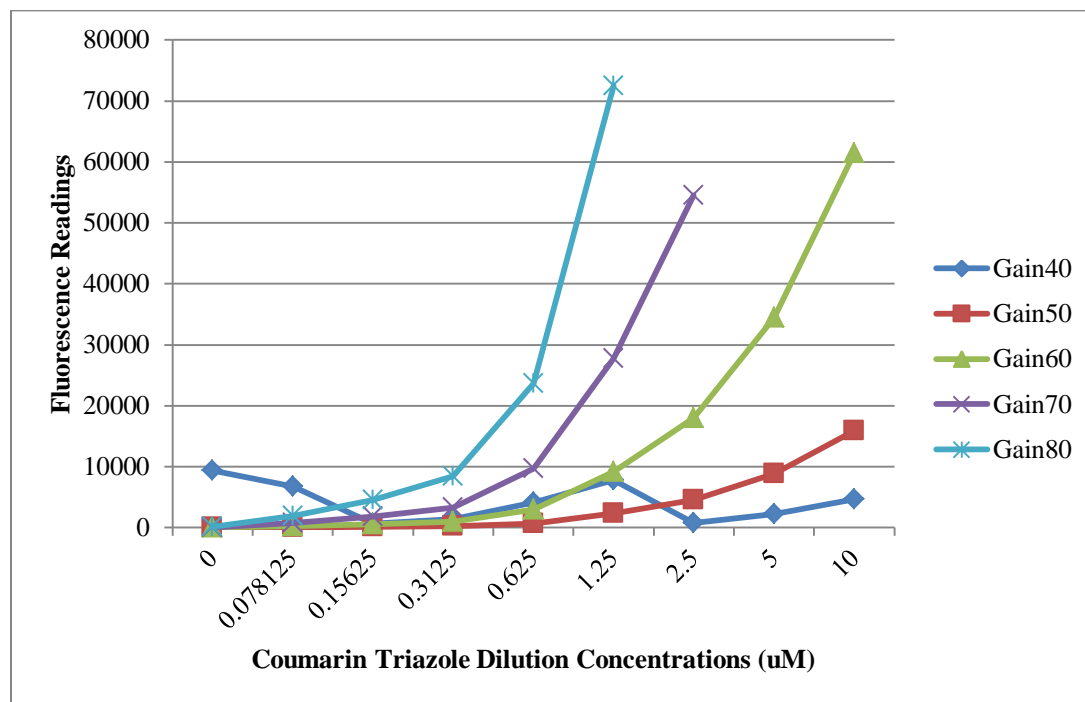
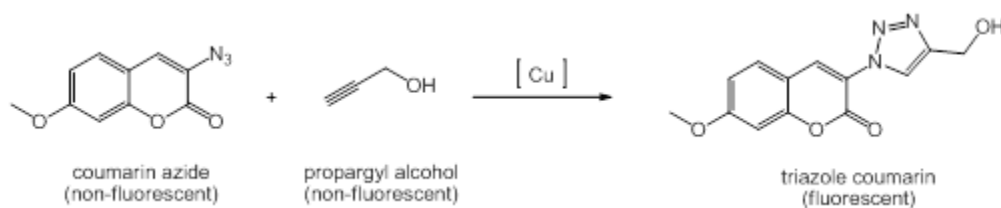


Figure 7: Gain Setting Calibration Readings





### Scheme 1: Click Chemistry Calibration

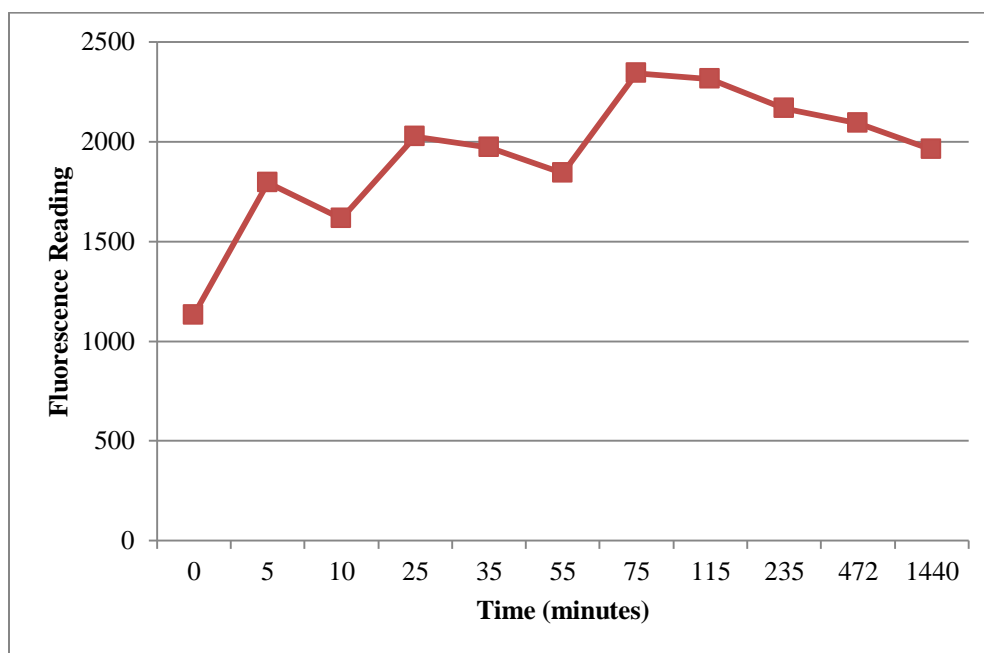
The calibration reaction was necessary to optimize reaction conditions for the click chemistry studies, which was important because only small amounts of ZIF-10 had been synthesized and purified for experimental study. Further, the data obtained from the calibration reaction were needed for use in quantifying the yield of future reactions.

There appear to have been some significant errors in technique or in plate reader measurement for the Gain40 calibration, given the irregularity of the curve. The curves for the Gain70 and Gain80 settings have fewer data points than the other curves because the higher concentrations yielded an “overflow” fluorescence value in the plate reader. This is why the Gain60 setting was optimal: it optimized the fluorescence readings for the selected dilution concentrations without any overflow.

**Table 4: Gain60 Setting Fluorescence Readings**

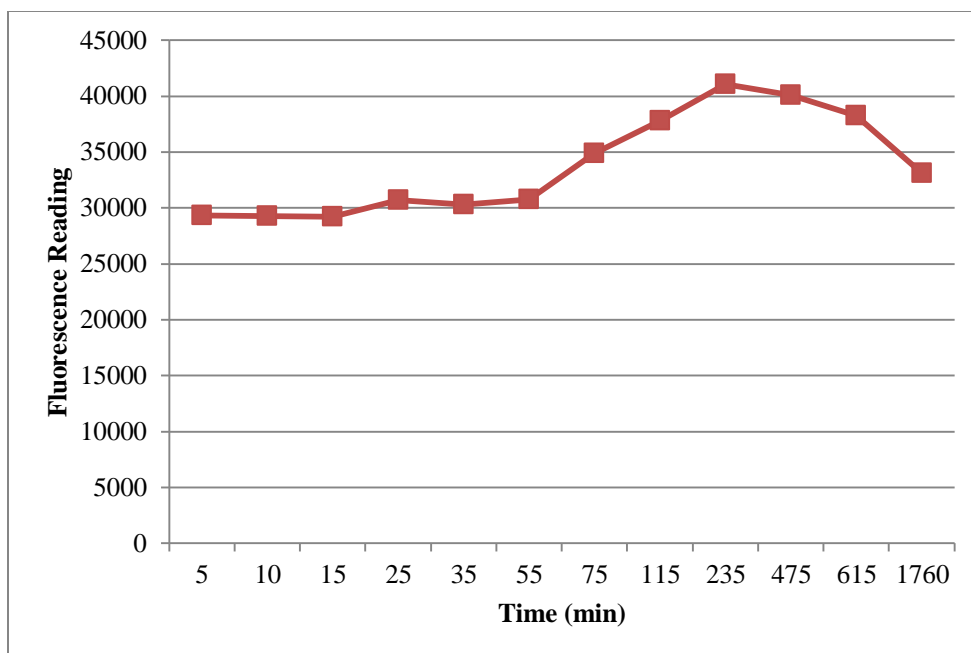
Concentration (uM)	Fluorescence Reading
0	14
0.078125	243
0.15625	541
0.3125	1030
0.625	2973
1.25	9142
2.5	18051
5	34462
10	61466

This table provides more detailed values for the fluorescence readings obtained during the Gain60 condition of the calibration trial. The data do not demonstrate any important trends, but they have been included here because these values were used to calculate the yield for the click chemistry reaction experiments. The full calculation procedure is described in the Experimental section.



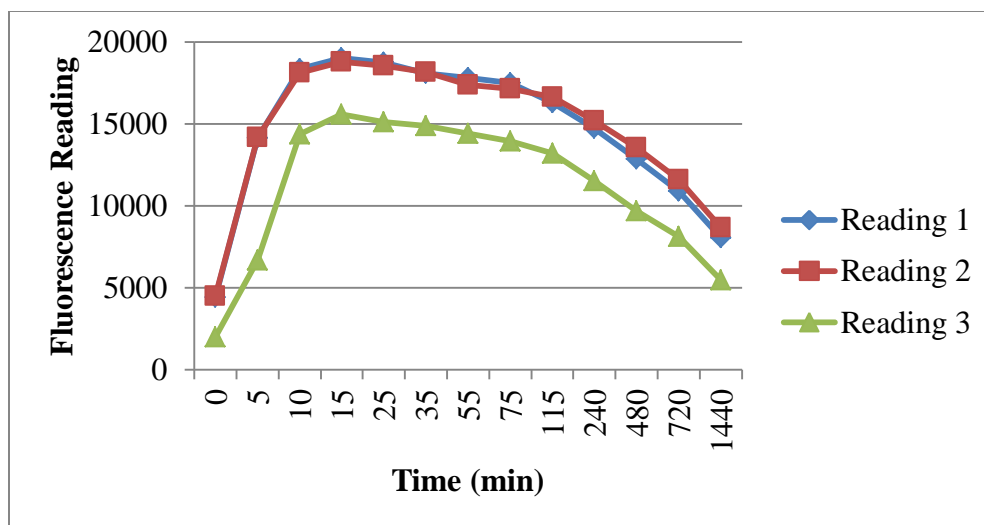
**Figure 8: Reaction #1, Literature Protocol without Ligand**

The first click chemistry reaction was performed between coumarin azide and propargyl alcohol (see Scheme 1). It was carried out without the THPTA ligand. The trend depicted in Figure 6 is best understood in the light of the other graphs showing the data from the click chemistry reactions (see Figures 8-10). As expected in a normal fluorescence curve, there is a clear peak in the reaction, which appears less than an hour and a half after the initiation of the reaction. It is not clear why the line is not smooth; it is unlikely that an issue with experimental technique was at play, given that the exact same technique was used for Reaction #2.



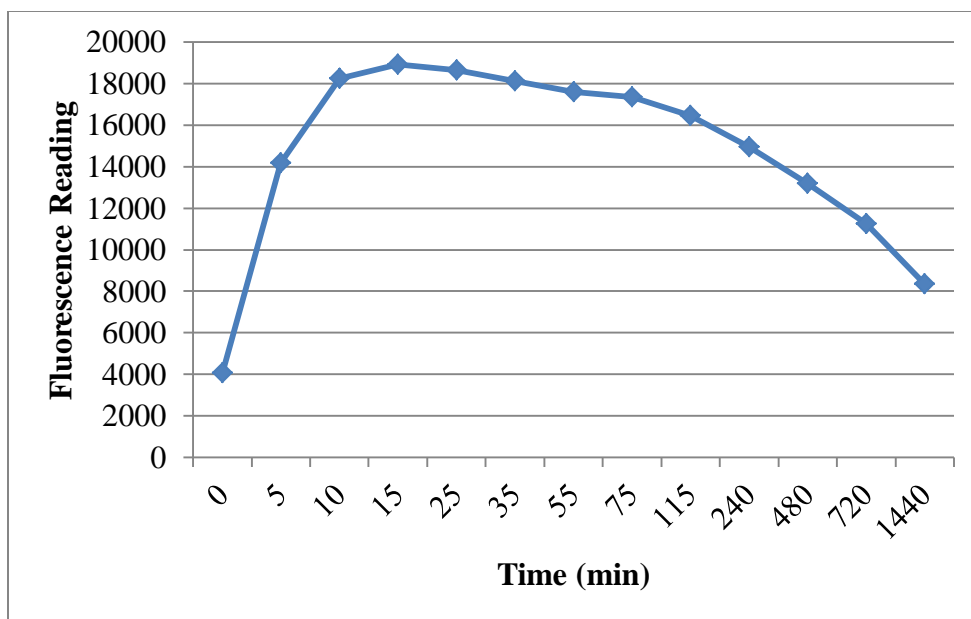
**Figure 9: Reaction #2, Literature Protocol with Ligand**

The second click chemistry reaction was identical to the components of the first click chemistry reaction except that it was carried out with a THPTA ligand. As seen in the trend in Figure 9 compared to that in Figure 8, the ligand not only significantly improved the intensity of the fluorescence readings obtained during the reaction monitoring (e.g. the peak in Reaction #2 is 41047, compared to 2345 in Reaction #1), but the peak of the reaction was also delayed by over two hours, which in the context of an indirect fluorescence imaging study would provide valuable time for more measurements to be taken. The trend line is much smoother than that in Figure 8, though they both do indicate a tapering decrease after the fluorescence peak, which will be discussed in detail in the Conclusions section. Ultimately, Reaction #2 demonstrates the great value and necessity of including the THPTA ligand in the reaction vessel.



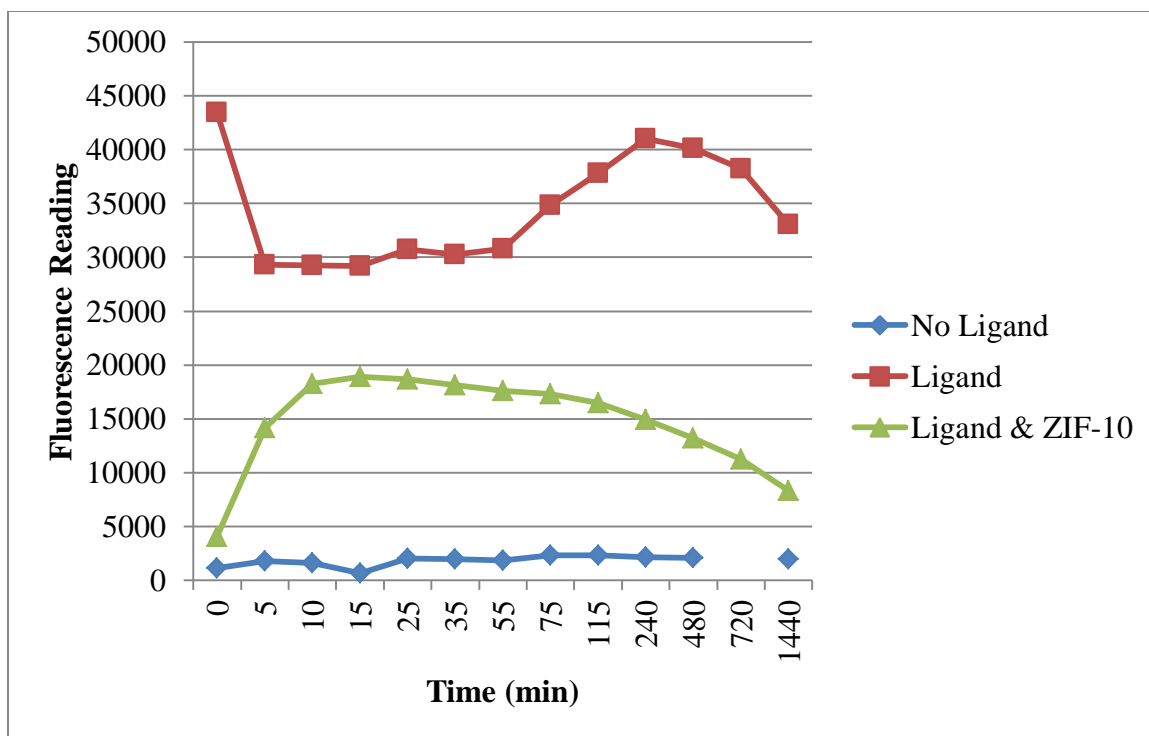
**Figure 10: Reaction #3, Zif-10 Study, Multiple Readings**

Figure 10 shows the data from three individual reaction wells collected during Reaction #3, the study reacting coumarin azide with ZIF-10 in the presence of the THPTA ligand. Because reading 3 is so much lower than the other two readings, it appears that there may have been an issue in the preparation of the third reaction well, for example the presence of bubbles that interfered with the fluorescence reading in the microplate reader. The peak fluorescence value in Reaction #3 occurred much earlier than it did in the other reactions: in less than half an hour, after which there is a gradual decline in fluorescence values than in the other reactions. Potential reasons for this decline will be discussed in the Conclusions section. The overall values for Reaction #3 are still higher than those in Reaction #1, but are lower than those in Reaction #2. Potential reasons for this will also be discussed in the Conclusions section.



**Figure 11: Reaction #3, Zif-10 Study, Average values**

In Figure 11 above, the values for readings 1 and 2 of the three measurements originally taken for the ZIF-10 study (Figure 10) were averaged at each time point. The third reading was not included because it was significantly lower than the first two readings and appeared to be the result of a technical error.



**Figure 12: Comparison of All Click Chemistry Reactions**

Figure 12 illustrates many of the points of comparison described below Figure 10.

The peak of Reaction #3 was much sooner than in the other two reactions and the subsequent decline in values is more gradual. The intensity of the fluorescence readings for Reaction #3 are also between those of the ligand-free Reaction #1 and Reaction #2 with the THPTA ligand.

**Table 5: Reaction #1 Yield**

Time (min)	Fluorescence Reading	% Yield
0	1132	3.29
5	1794	4.35
10	1614	4.06
25	2025	4.73
35	1971	4.64
55	1842	4.43
75	2345	5.24
115	2316	5.19
235	2167	4.95
472	2095	4.84
1440	1962	4.62

The values of the fluorescence readings at each time point were used to calculate the percentage yield of the reaction, using a specific formula described in the Experimental section. As discussed below Figures 8 through 12, the fluorescence intensity was the lowest for Reaction #1. The yield was also by far the lowest, its peak being 5.24% at the fluorescence peak of the reaction, 75 minutes.

**Table 6: Reaction #2 Yield**

Time (min)	Fluorescence Reading	% Yield
5	29323	42.17
10	29264	42.08
15	29208	41.99
25	30723	44.30
35	30280	43.63
55	30776	44.38
75	34861	50.74
115	37814	56.21
235	41047	62.19
475	40108	60.45
615	38246	57.01
1760	33085	47.90

Compared to the data in Table 5, it becomes clear that the presence of the THPTA ligand is essential to maximize fluorescence intensity as well as to improve the yield of the click chemistry reaction. It is not clear whether the ligand is responsible for the delay in the peak, given that the peak in Reaction #3 is even earlier than that of Reaction #1, even though a ligand was used in Reaction #3.

**Table 7: Reaction #3 Yield**

Time	Average Reading	% Yield
0	4058.75	7.35001
5	14169	19.5533
10	18250.5	25.3039
15	18912	26.3116
25	18654.5	25.9194
35	18134	25.1264
55	17597	24.363
75	17335	23.9954
115	16469	22.7803
240	14950.5	20.6498
480	13205	18.2007
720	11260	15.4717
1440	8354.5	11.7022

Similar to the other reactions, the peak in the yield occurs at the peak fluorescence intensity reading in Reaction #3. This occurs at the 15 minute time point, which is significantly earlier than the peak occurred in the two earlier reactions. The yield and fluorescence intensity are also not as high as could be anticipated, given the presence of the ligand and the data collected from Reaction #2. Potential reasons for this will be discussed in the Conclusions section.



## Conclusions

Ipomoeassin F is one member of a small group of resin glycosides derived from the leaves of the morning glory flower, *ipomoea squamosa*. It is of great interest to researchers because of its impressive potency against many lines of cancer cells, and stands out among other ipomoeassins as being the most potent against all cell lines currently tested (Cao, et al., 2007). However, all that is currently known about ipomoeassin F is its cytotoxicity to cancer cells.

This study sought to begin exploring the mode of action of ipomoeassin F via fluorescence imaging studies, to investigate the cellular localization. Towards the goal of a direct fluorescence imaging study, a BODIPY dye probe was synthesized to ultimately attach to ipomoeassin F. The yield was very poor, averaging a total of 0.46% yield for the full synthetic route, and the products were not completely pure. However, even if the yield were perfect it was found through structure-activity relationship (SAR) studies and cytotoxicity assays that a BODIPY-tagged ipomoeassin F analog could not have been used to study ipomoeassin F's mode of action. This was seen in the significantly-higher  $IC_{50}$  values for both ZIF-4 and ZIF-5 (see Figure 5), which are structurally representative of a BODIPY-tagged ipomoeassin F analog (see Table 3 and Figure 6).

Because the  $IC_{50}$  value is 119 and 148 times higher for the two analogs, respectively, compared to unmodified ipomoeassin F, it is obvious that the chemical alteration that would be required to attach a BODIPY dye probe would profoundly alter the normal cytotoxic abilities of the molecule. To study a tagged analog would not even be representative of ipomoeassin F's mode of action, and so it was not even worth

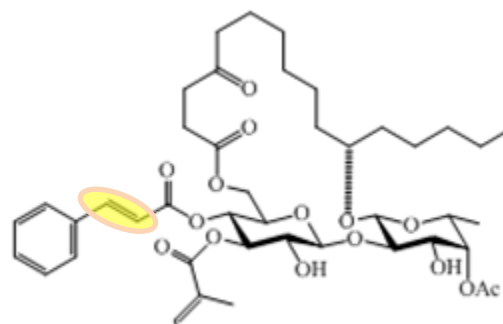


**Figure 13: The Critical Double Bond**

attempting. However, important knowledge was still obtained regarding the mode of action through this failed application. Through deductive reasoning it was seen that the key structural difference between ZIF-4/ZIF-5 and ipomoeassin F is the lack of the double bond adjacent to the benzene ring (see Figure 13), and thus this double bond appears to be critical to the chemical function of ipomoeassin F.

ZIF-9, an ipomoeassin F analog (see Figure 5) tagged by another fluorescent probe, coumarin, was provided by a post-doctoral fellow and investigated here for its suitability as a means to study ipomoeassin F's mode of action. The cytotoxicity assays performed as part of this study revealed that ZIF-9, too, was 1449 times less potent against MDA-MB-231 cancer cells, and so it was unsuitable for fluorescence imaging studies as well (see Table 3). From these results, it is clear that at least with the particular dye probes in use, direct fluorescence imaging of ipomoeassin F is not possible. However, further mechanistic information was gleaned from the investigation of coumarin as well. Initially it was believed that because of the structural similarities between coumarin and the cinnamate moiety on ipomoeassin F (see Figure 2), that a

coumarin-tagged probe would have minimal functional disturbances. This belief was disproved. But this led to some contemplation of any remaining differences between coumarin and the cinnamate moiety, and it was determined that although the coumarin rings are flat, the benzene ring and double bond in the cinnamate moiety could be at an angle to each other in the binding pocket. Because its absence leads to a severe disruption in cytotoxic abilities, it appears that this feature is also necessary for the mode of action of ipomoeassin F. Though this information is of course valuable, ultimately the use of BODIPY and coumarin failed to meet the needs of this investigation; therefore, indirect fluorescence imaging via click chemistry was explored.

It should be noted that this investigation—largely due to time constraints after dedicating months to synthesizing and investigating BODIPY and coumarin’s potential—is a very preliminary study with regards to indirect fluorescence imaging. The major progress made here is that the proper conditions for study were established, in addition to the discovery of several considerations for future consideration.

First, the calibration titration established that the optimal Gain setting for the microplate reader was 60 (see Scheme 1 and Figure 7). The calibration reaction also provided intensity readings at various concentrations that were utilized in future percent yield calculations for the three click chemistry reactions (see Table 4), describing the correlation between fluorescence readings and concentrations of the fluorescent product. The first and second click chemistry reactions were performed as a model system for future indirect fluorescence imaging studies, in that they combined the coumarin azide with a much simpler propargyl alcohol, rather than the alkyne in ZIF-10 used in the third reaction. Together, they demonstrated the necessity of the presence of the THPTA ligand,

which improved the percentage yield of the click chemistry reaction over tenfold (see Tables 5 and 6). The final click chemistry reaction performed with ZIF-10— the molecule of interest due to its similar cytotoxicity profile to unmodified ipomoeassin F— demonstrated mostly several trends that must be considered in future endeavors towards indirect fluorescence imaging studies of ipomoeassin F. The yield was lower than expected compared to the second click chemistry reaction (see Table 7 and Figure 12), but it is thought that this is because the model system is not as representative as initially believed. Not only could this lead to overly optimistic expectations of the yield of the reaction, but any yield calculations could be false as well, since they were based readings from the calibration reaction that also relied on the model of the propargyl alcohol. There was also a question of why the fluorescence intensity began to decline in all of the click chemistry reactions—i.e. excluding the calibration titration—, rather than just plateauing. A recent publication may have provided the answer. It was found that the presence of copper (which in this study was present as copper (II) sulfate pentahydrate in both the model systems and the ZIF-10 study, but not in the calibration titration) promotes the degradation of the fluorophore under aerobic conditions, which would lead to the declining fluorescence intensity that was observed (Helan, Gulevich, & Gevorgyan, 2015).

Future investigations based on the research described here could largely focus on improving and expanding upon the work towards indirect fluorescence imaging to obtain cellular localization information. First, the problem of the copper digestion needs to be solved. It is perhaps possible that the copper could be removed near the peak of the reaction to prevent fluorophore digestion, or some other “decoy” ingredient could be

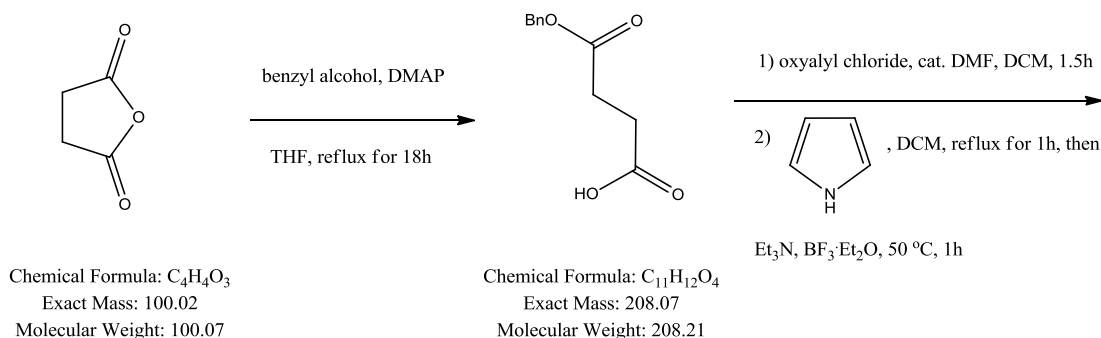
added to the system to prevent the digestion by binding the copper instead of the fluorophore. Next, full studies to evaluate the cellular localization of ipomoeassin F can be performed. It is also possible to expect that direct fluorescence imaging could be performed with other probes, though it has been shown here that it will be impossible with BODIPY and coumarin in particular.

## **Experimental Materials and Methods**

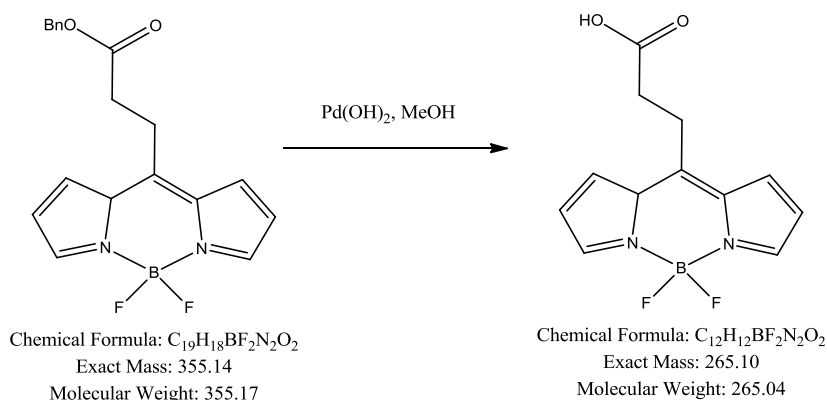
All reagents and solvents that were utilized for the synthetic chemical reactions were obtained from commercial sources. Chemical shifts for  $^1\text{H}$  and  $^{13}\text{C}$  NMR spectra were obtained using deuterated chloroform, using a Bruker 400 MHz NMR spectrometer.

### **BODIPY Synthesis**

The synthesis of the 3-(4,4-difluoro-1,3,5,7-tetramethyl-4-bora-3a,4a-diaza-s-indacene-8-yl)-propionic acid, or BODIPY, dye was performed according to the one-pot synthesis (Pathway 1) described in the 2009 paper by Machida and colleagues, and represented by the pathway below (Machida, Tsubamoto, Kato, Harada, & Ohkanda, 2013). There were multiple attempts to complete the three major steps of this reaction, to the end of obtaining enough for potential fluorescence imaging experiments.

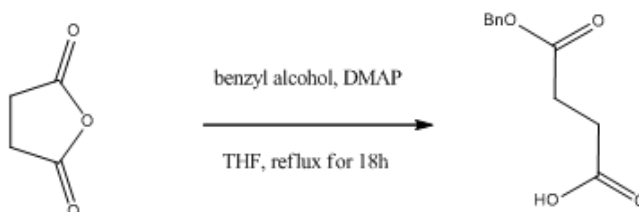


succinic anhydride



## Scheme 2: Full Synthetic Pathway for BODIPY

To begin the first step, succinic anhydride (1.0 gm, 10 mmol), anhydrous DMAP (54 mg, 0.44 mmol), and benzyl alcohol (1.14 g or 1.1 mL, 11 mmol) were combined in approximately 10 mL of THF. The mixture was charged with nitrogen gas—to prevent the succinic anhydride from reacting with water in air rather than with the benzyl alcohol—and refluxed at 81° C for 18 hours, at which point a work-up was performed. Sodium bicarbonate was added to react with any remaining free carboxylic acid for 20 minutes, at which point ethyl acetate was added to form an organic and aqueous layer. The organic layer—the top layer—was discarded. Hydrochloric acid was added

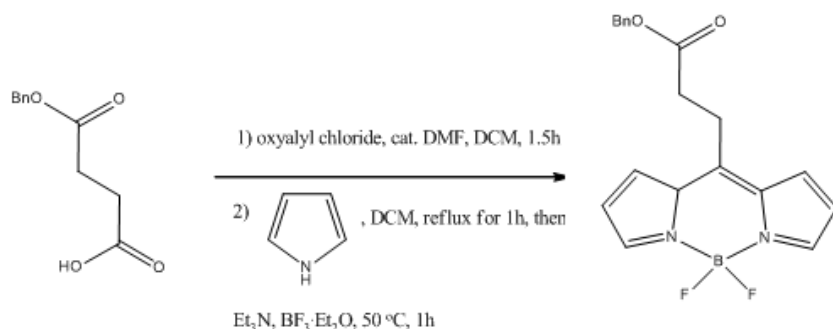


Scheme 3: BODIPY Synthesis Step 1

to acidify the reaction, to convert all carboxylic acid salt—formed as a result of the addition of sodium bicarbonate—back into carboxylic acid. Once the pH was gauged to be 2 using Litmus paper—after adding over 8 mL of HCl—and gas bubbles no longer formed, the organic layer was extracted. To the organic layer, anhydrous sodium sulfate was used to remove any remaining water in the mixture. The product was then filtered through cotton to preserve the liquid contents. The solvent was then removed via evaporation, a small amount of hexane was added, and the contents were left overnight to recrystallize. The crystalline product was isolated later using vacuum filtration, yielding succinic acid monobenzyl ester.

The second step required mixing the succinic acid monobenzyl ester (1.02 g, 4.9 mmol), oxalyl chloride (1.65 g, 13 mmol), and a catalytic amount of DMF in 40 mL of DCM in dry conditions, charged with nitrogen gas. The reaction took place over 1.5 hours at room temperature. The solvents were evaporated out of the container to concentrate the products. To the products, a solution of pyrrole (0.4898 g, 0.51 mL, 7.3 mmol) in 20 mL of dry DCM was added, and refluxed for 1 hour at 55° C. The reaction was then quenched and cooled to room temperature. Then trimethylamine (3.5 mL, 25 mmol) in approximately 32 mL of toluene and boron trifluoride diethyl ether (3.1 mL, 25 mmol) were added, and stirred while the mixture reacted for 1 hour at 50° C. Afterwards, the products were

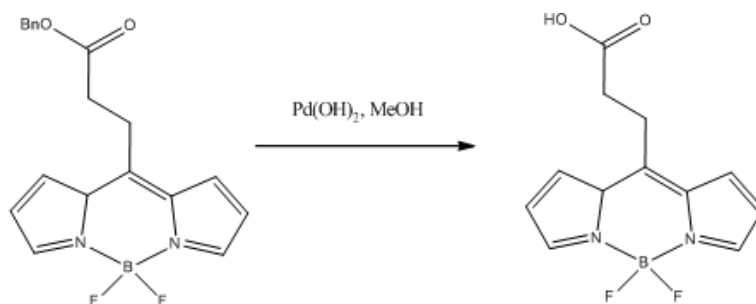
purified via extraction  
with dichloromethane  
followed by silica gel



**Scheme 4: BODIPY Synthesis Step 2**

column chromatography.

For the third and final step, the products of the second step (112 mg, 0.27 mmol) underwent a

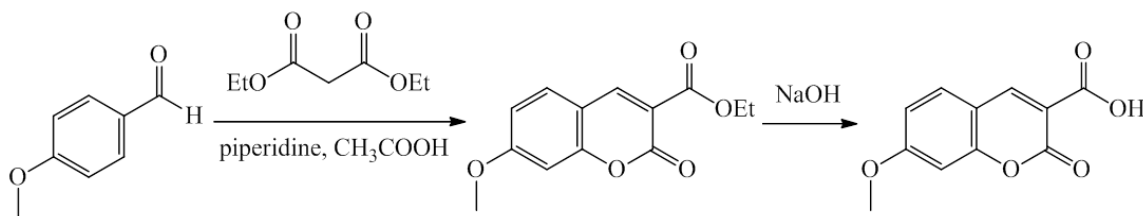


**Scheme 5: BODIPY Synthesis Step 3**

hydrogenation reaction with palladium hydroxide in methanol to yield the final desired product: 3-(4,4-difluoro-1,3,5,7-tetramethyl-4-bora-3a,4a-diaza-s-indacene-8-yl)-propionic acid, or BODIPY free acid.

### Coumarin Synthesis

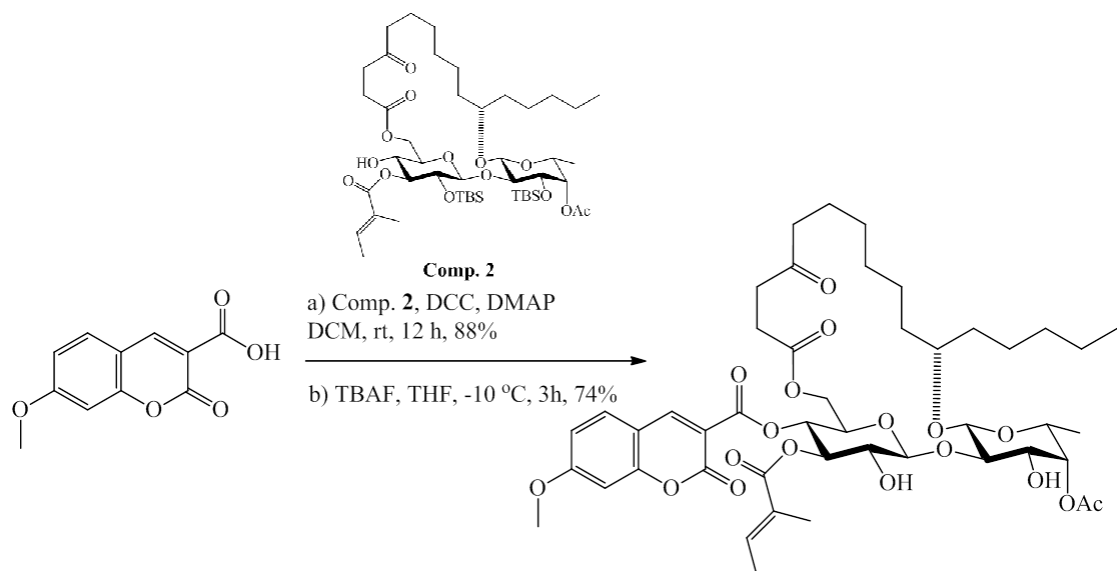
Coumarin was synthesized (Scheme 6) in the Shi laboratory by a postdoctoral fellow, Dr. Mugunthan Govindarajan. It followed the synthetic pathway given below, as described in existing literature.



**Scheme 6: Synthetic Pathway for Coumarin**

Dr. Guanghui Zong, another postdoctoral fellow, attached the coumarin moiety to ipomoeassin-F to form a labeled analog that was named ZIF-9, according to the pathway below.





**Scheme 7: Synthesis of ZIF-9**

### Cytotoxicity Assays of ipomoeassin F and analogs

The cytotoxicity assays performed for these experiments tested the potency of several analogs of ipomoeassin F (see Figure 6), in addition to unmodified ipomoeassin F as it was synthesized. Their structures are listed in Figure 5. ZIF-4 and ZIF-5 are analogs of ipomoeassin F that have been modified in such a way that mirrors the modifications entailed in the tagging of ipomoeassin F with BODIPY. They were used rather than a BODIPY-tagged analog because they had already been synthesized as part of an existing library of ipomoeassin F analogs being created in the Shi lab. ZIF-9 is a coumarin-labeled analog. ZIF-10 is an analog tagged with a biorthogonal alkyne group rather than a fluorescent dye. Ipomoeassin F was utilized as a comparative positive control to observe any deleterious effects of adding moieties to the ipomoeassin F molecule, and Taxol was utilized as a positive control for efficacy of the treatments as compared to a current industry standard treatment.

All cytotoxicity assays were performed using the MDA-MB-231 human metastatic breast cancer cell line, which were cultured in an FBS serum with 10% penicillin streptomycin. Most cell culture and maintenance outside of the assay test periods was performed by a postdoctoral fellow in the lab, Dr. Hazim Al-Jewari.

The cytotoxicity assay takes place over a 5-day period, with activity required on the first, second, and fifth days. On the first day a 96-well plate was prepared using FBS media the cultured cells at a density of  $5 \times 10^4$  cells per well. The wells in each of the four corners of the plate were left completely empty until the final day of the assay schedule. The other wells in the outermost rows and columns of the plate were filled only with equivalent amounts of FBS media, to protect the cell-containing wells from the effects of media evaporation during incubation. The plate was then incubated at 37° C and 5% CO<sub>2</sub> for 24 hours.

On the second day, stock solutions of the compounds desired for testing on the 96-well plate were prepared and inserted into the cell-containing wells. Over the following 72 hours the solutions would have time to demonstrate their effect on the cells, ideally by killing them. Prior to adding the treatment solutions, it was ensured that the volume of media in all the wells was equivalent. Typically one small section of the plate (e.g. 4 – 7 wells) was assigned to be a negative control, and at least one other section was treated with ipomoeassin F and/or Taxol to serve as (a) positive control(s). The plate was then incubated at 37° C and 5% CO<sub>2</sub> for 72 hours. Changes in cell morphology and density were monitored each day during this 72-hour span. For sample photos, see Appendix B.

On the fifth day of the assay time schedule, the AlamarBlue dye was used to make the fluorescence readings indicating the efficacy of the treatments used. An AlamarBlue stock solution was used for all cytotoxicity assay experiments, containing 3 mg in 27.15 mL. To start, 180  $\mu$ L of the AlamarBlue dye was added to each of the four corner wells, to serve as controls for “background” fluorescence in the data analysis. Then 20  $\mu$ L of AlamarBlue dye was added to all other wells. The plate was returned to the incubator for 4.5 hours at 37°C and 5% CO<sub>2</sub>. During the incubation period, healthy cells are able to absorb and metabolize the dye via reduction that neutralizes the fluorescence, but dead or dying cells retain the dye without modification. To evaluate the proportion of cells retaining the dye, the fluorescence reading was taken using a Biotek microplate reader at 580 nm (excitation) and 620 nm (emission) wavelengths. The measurements typically needed to be repeated three to six times to obtain consistent, properly calibrated readings. The fluorescence data was then used to calculate the percentage of dead cells resulting from the treatments, which was in turn used to calculate IC<sub>50</sub> values for the treatments.

### **Click Chemistry Reactions**

The purpose of the click chemistry reaction was to join the ZIF-10 analog with another molecule that, together, would be fluorescent—a fluorogenic reaction. Using the combined molecule, fluorescence imaging studies were then performed in fixed cells with a confocal microscope. This study conducted three click chemistry reactions, plus one calibration titration, to optimize the reaction conditions and provide a standard of comparison for calculating yield. The protocol for the non-calibration reactions is based on the 2013 paper by Luo and colleagues (Luo, Tikekar, & Nitin, 2013).

**Calibration titration.** The calibration titration was performed to evaluate which plate reader settings would be helpful in obtaining optimum measurements in the future click chemistry reaction experiments. Beginning with a 10  $\mu\text{M}$  stock solution of coumarin triazole, wells were filled in a 96-well plate such that the concentration decreased progressively across the wells. The upper left well was filled with a 0.1 M Triton buffer (pH = 8.5, 0.05% Triton) to use as a baseline control. Starting at 10  $\mu\text{M}$ , the solution was diluted by half in each well until it was at a 0.078  $\mu\text{M}$  concentration. Nine wells in total were used on the plate.

The fluorescence of the plate was measured at an excitation wavelength of 404 nm, and an emission wavelength of 477 nm—which were optimized by another undergraduate researcher in the lab. The read height of the plate reader was 7 mm. The plate was read five times with various Gain settings: once each at a setting of 40, 50, 60, 70, and 80. Based on the results, the optimum Gain setting was selected and used for the other click chemistry reactions as a comparison.

**Calculation of Click Chemistry Reaction Yield.** First, each reading was compared to the readings of the Gain60 calibration reaction (see Table 4). For a given experimental reaction reading,  $x$ , the concentration of the nearest calibration reading value larger than  $x$ ,  $q$ , and the concentration of the nearest calibration reading value smaller than  $x$ ,  $p$ , were identified. The readings at the larger calibration concentration and the smaller calibration concentration were  $a$  and  $b$ , respectively. The following formula was then used to calculate the percentage yield:  $\left(p + (q - p) * \frac{x - b}{a - b} * 100\right) / 10$ .

**Click Chemistry Reaction #1: Literature protocol without ligand.** In one reaction vessel, 50  $\mu\text{L}$  of copper (II) sulfate pentahydrate (24.9 mg, 1mM), 50  $\mu\text{L}$  of propargyl alcohol (10  $\mu\text{M}$ ), 50  $\mu\text{L}$  of L-ascorbic acid sodium salt (198 mg, 50 mM), and 50  $\mu\text{L}$  of coumarin triazole (10  $\mu\text{M}$ ) were combined in 4800  $\mu\text{L}$  of the 0.1 M Triton buffer. The reaction was carried out at room temperature for 24 hours, stirring constantly. A timer was started the moment the first 20  $\mu\text{L}$  sample was removed for the first reading, to identify the time points for fluorescence measurements to take place. Measurements were taken using the plate reader at 0, 5, 10, 15, 25, 35, 55, 75, 115, 235, 475, and 1440 minutes.

**Click Chemistry Reaction #2: Literature protocol with ligand.** In one reaction vessel, 50  $\mu\text{L}$  of copper (2) sulfate pentahydrate (24.9 mg, 1mM), 50  $\mu\text{L}$  of propargyl alcohol (10  $\mu\text{M}$ ), 50  $\mu\text{L}$  of L-ascorbic acid sodium salt (198 mg, 50 mM), 50  $\mu\text{L}$  of coumarin azide (10  $\mu\text{M}$ ), and 30  $\mu\text{L}$  of a THPTA ligand in DMSO (6 mM) to improve the copper sulfate pentahydrate's function were combined in 4770  $\mu\text{L}$  of 0.1 M Triton buffer. The reaction was carried out at room temperature for 24 hours, stirring constantly. A timer was started the moment the first 20  $\mu\text{L}$  sample was removed for the first reading, to identify the time points for fluorescence measurements to take place. Measurements were taken using the plate reader at 0, 5, 10, 15, 25, 35, 55, 75, 115, 235, 475, 600, and 1440 minutes.

**Click Chemistry Reaction #3: ZIF-10 Study.** In one reaction vessel, 6  $\mu\text{L}$  of copper (2) sulfate pentahydrate (1mM), 0.6  $\mu\text{L}$  of ZIF-10 (10  $\mu\text{M}$ ), 6  $\mu\text{L}$  of L-ascorbic acid sodium salt (50 mM), 6  $\mu\text{L}$  of coumarin azide (10  $\mu\text{M}$ ), and 36  $\mu\text{L}$  of a THPTA ligand in DMSO (6 mM) were combined in 545.4  $\mu\text{L}$  of 0.1 M Triton buffer for a total volume of 600  $\mu\text{L}$ . The total volume of the reaction mixture was divided equally between three wells in a 96-

well plate, and the fluorescence of each well was measured to provide more data. The reaction was carried out at room temperature for 24 hours, placed in a shaker between measurements. A timer was started the moment the first fluorescence measurement was completed. Unlike the other two click chemistry reactions, no volume was removed for measurement; the reaction vessel itself was measured because the reaction was taking place in the 96-well plate to begin with. Measurements were taken using the plate reader at 0, 5, 10, 15, 25, 35, 55, 75, 115, 235, 475, 600, and 1440 minutes.

## References

- Cao, S., Norris, A., Wisse, J. H., Miller, J. S., Evans, R., & Kingston, D. I. (2007, August). Ipomoeassin F, a new cytotoxic macrocyclic glycoresin from the leaves of *Ipomoea squamosa* from the Suriname rainforest. *Natural Product Research*, 21(10), 872-876. doi:10.1080/14786410600929576
- Giessler, K., Griesser, H., Gohringer, D., Sabirov, T., & Richert, C. (2010, July). Synthesis of 3'-BODIPY-Labeled Active Esters of Nucleotides and a Chemical Primer Extension Assay on Beads. *European Journal of Organic Chemistry*, 2010(19), 3611-3620. doi:10.1002/ejoc.201000210
- Helan, V., Gulevich, A. V., & Gevorgyan, V. (2015, January). Cu-catalyzed transannulation reaction of pyridotriazoles with terminal alkynes under aerobic conditions: efficient synthesis of indolizines. *Chemical Science*, 6(3), 1928-1931. doi:10.1039/C4SC03358B
- Kolb, H. C., Finn, M. G., & Sharpless, K. B. (2001, June). Click Chemistry: Diverse Chemical Function from a Few Good Reactions. *Angewandte Chemie International Edition*, 40(11), 2004-2021. doi:10.1002/1521-3773(20010601)40:11<2004::AID-ANIE2004>3.0.CO;2-5
- Luo, Z., Tikekar, R. V., & Nitin, N. (2013, December). Click Chemistry Approach for Imaging Intracellular and Intratissue Distribution of Curcumin and Its Nanoscale Carrier. *Bioconjugate Chemistry*, 25, 32-42. doi:10.1021/bc4002008
- Machida, S., Tsubamoto, M., Kato, N., Harada, K., & Ohkanda, J. (2013). Peptidomimetic modification improves cell permeation of bivalent farnesyltransferase inhibitors. *Bioorganic & Medicinal Chemistry*, 21, 4004-4010. doi:10.1016/j.bmc.2012.09.061
- Newman, D. J., & Cragg, G. M. (2012, February). Natural Products As Sources of New Drugs over the 30 Years from 1981 to 2010. *Journal of Natural Products*, 75(3), 311-335. doi:10.1021/np200906s
- Ulrich, G., Ziesel, R., & Harriman, A. (2007, December). The Chemistry of Fluorescent Bodipy Dyes: Versatility Unsurpassed. *Angewandte Chemie International Edition*, 47(7), 1184-1201. doi:10.1002/anie.200702070
- Zhu, S.-Y., Huang, J.-S., Zheng, S.-S., Zhu, K., & Yang, J.-S. (2013, July). First Total Synthesis of the Proposed Structure of Batatin VI. *Organic Letters*, 15(16), 4154-4157. doi:10.1021/ol4020255

## Appendix A: NMR Spectra for BODIPY Synthetic Products

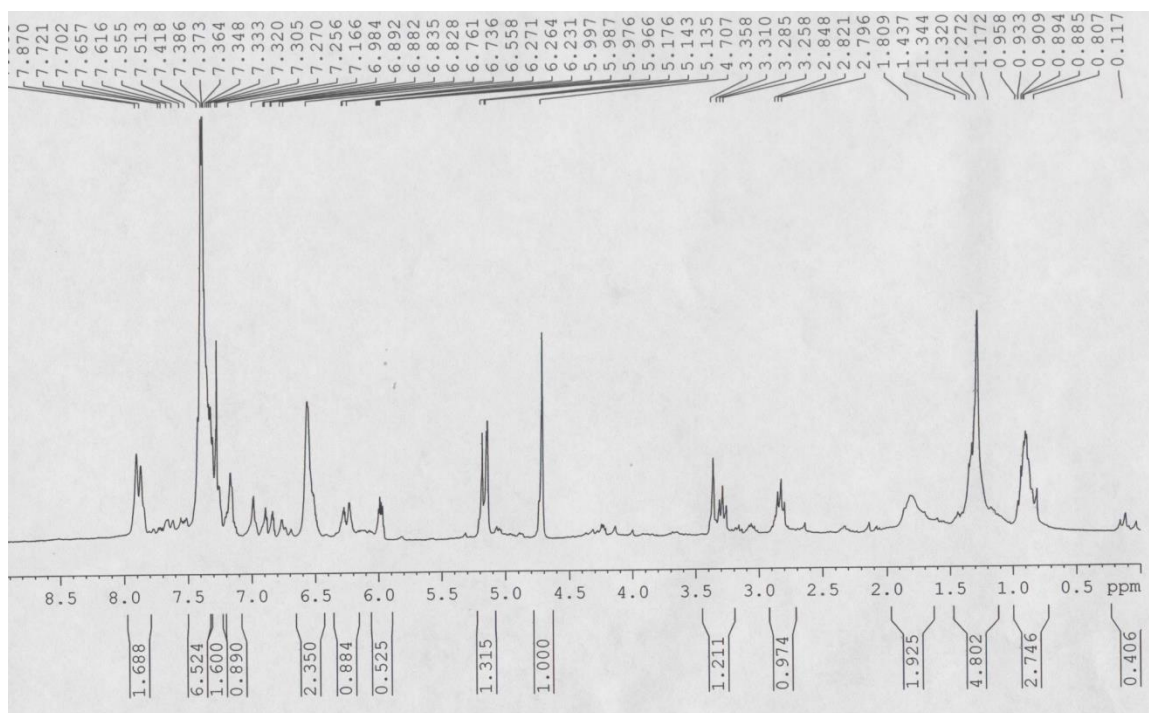


Figure 14: Proton NMR of Attempt 1 Final Product

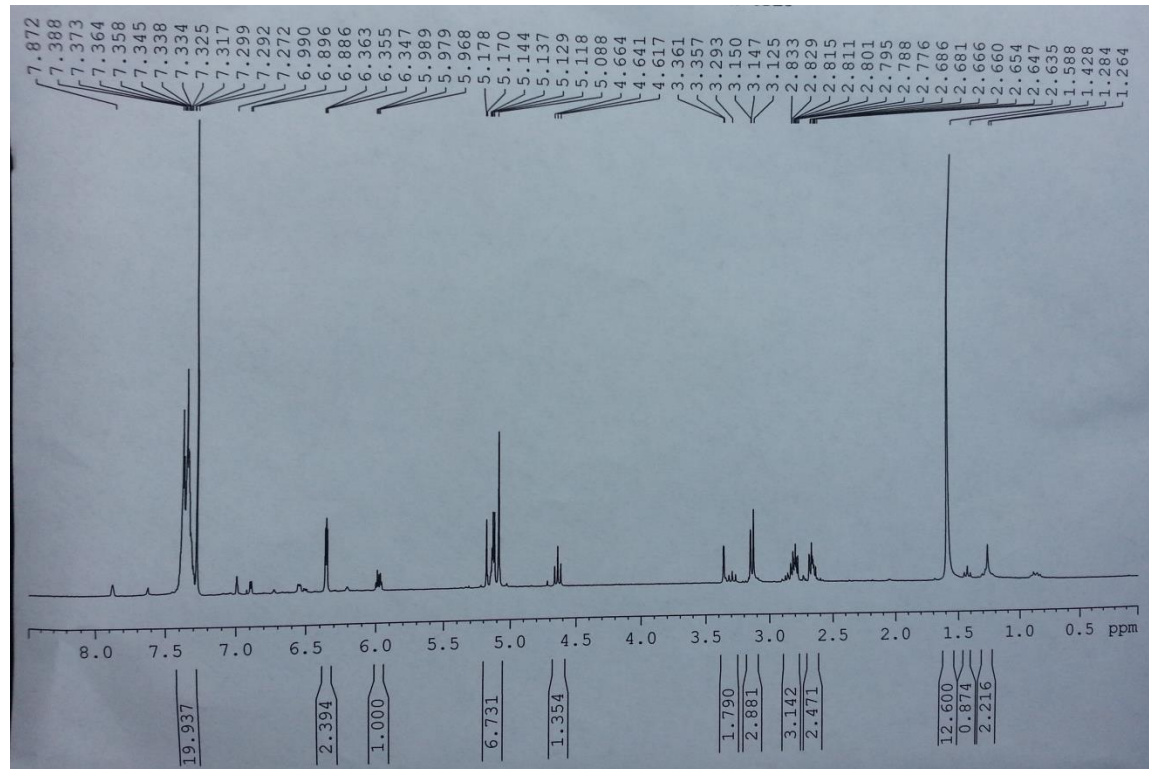
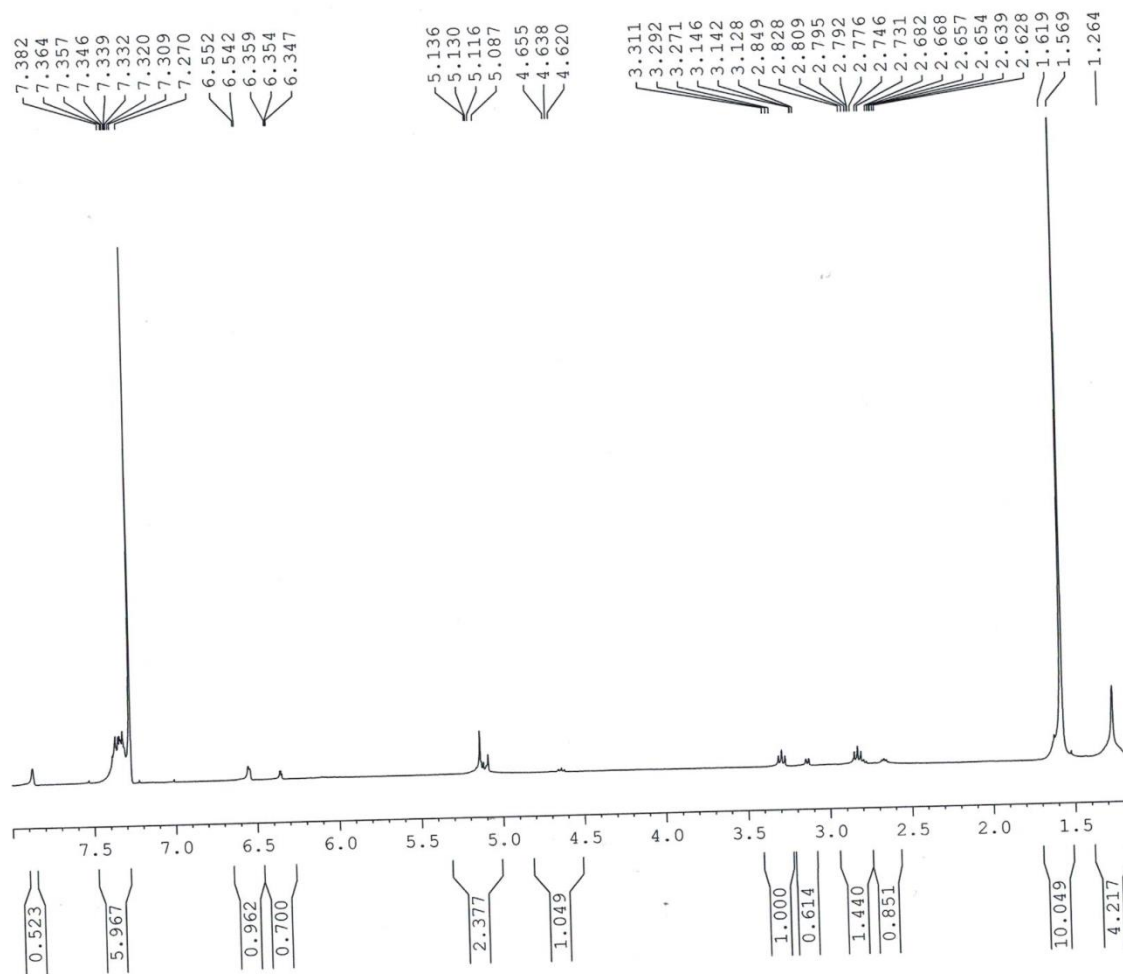
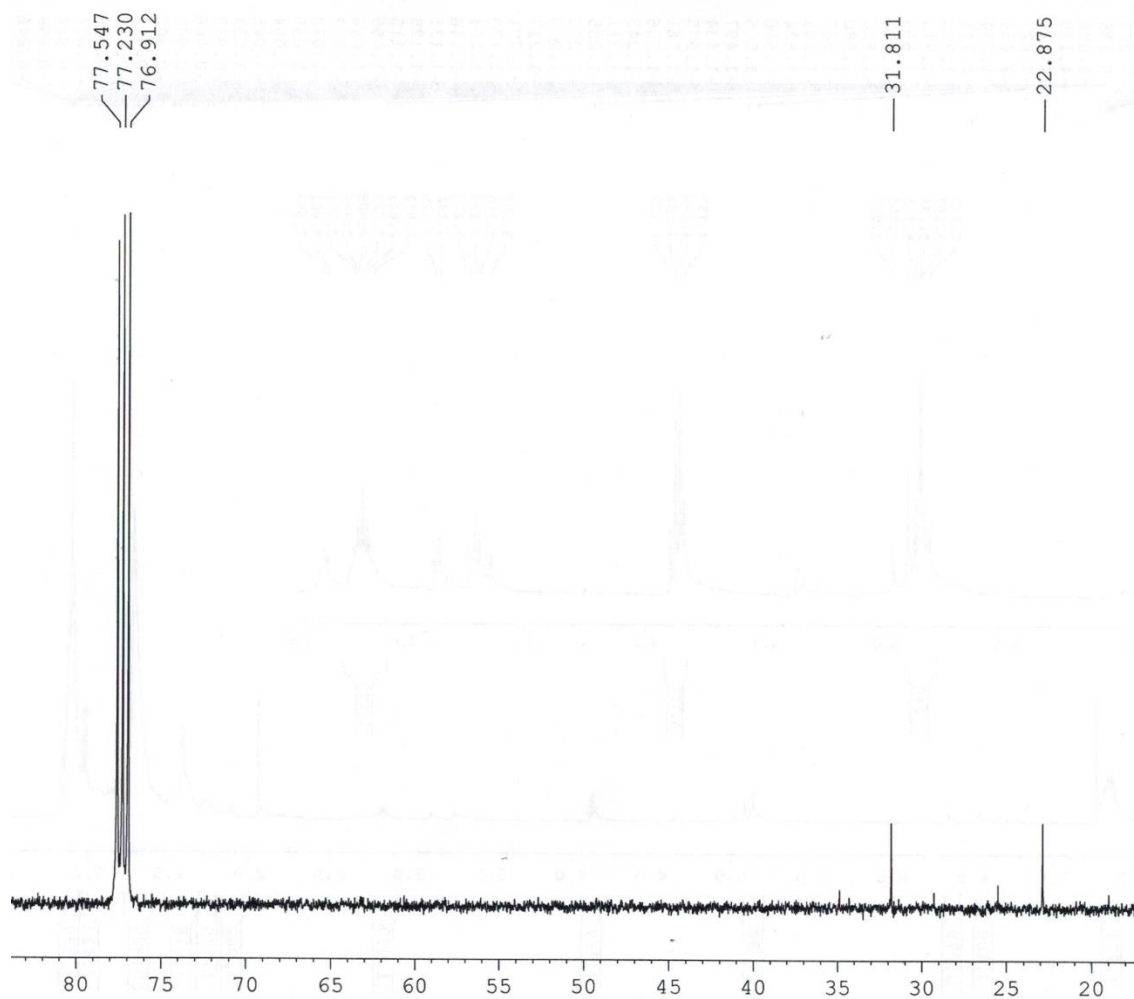


Figure 15: Proton NMR of Attempt 2 Final Product



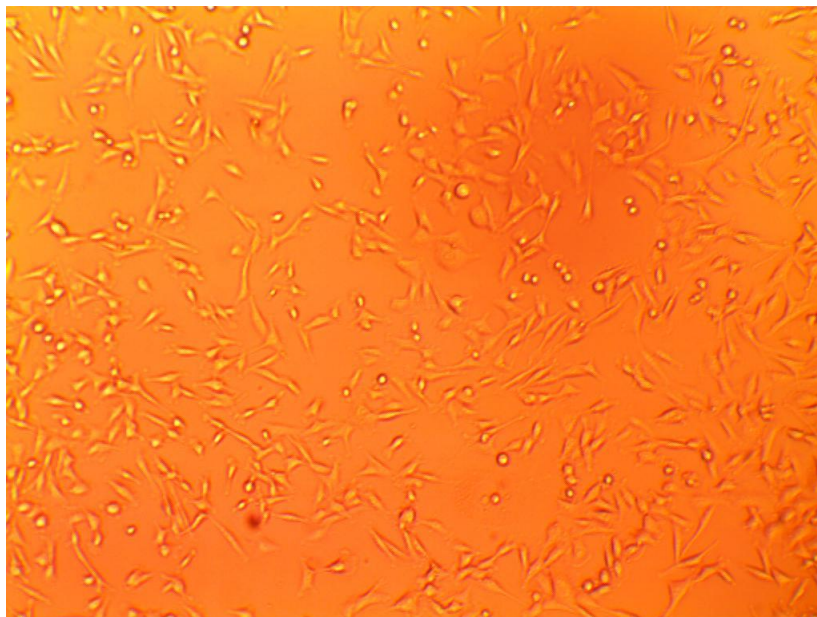


**Figure 16: Proton NMR of Attempt 3 Final Product**



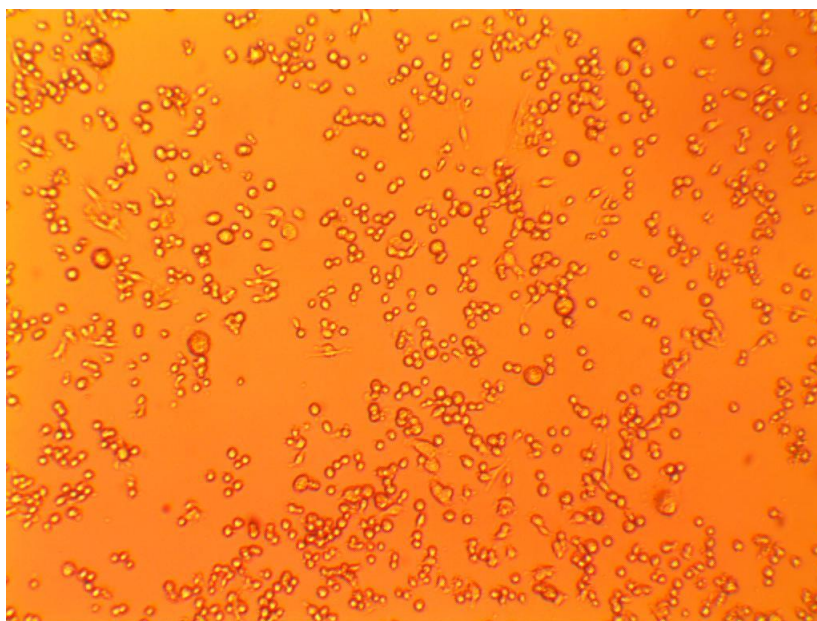
**Figure 17: Carbon NMR of Attempt 3 Final Product**

## Appendix B: Sample Cell Morphology Photographs



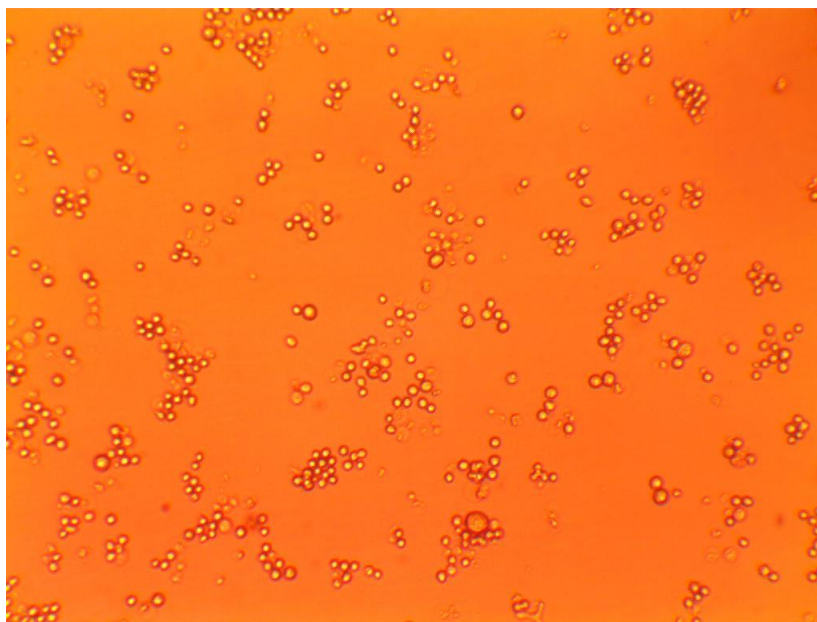
**Figure 18: Untreated MDA-MB-231 cells, cultured for 72 hours**

Photo credit: Dr. Hazim Al-Jewari



**Figure 19: 7.8 nm ZIF-10, cultured in MDA-MB-231 for 72 hours**

Photo credit: Dr. Hazim Al-Jewari



**Figure 20: 1000 nm ZIF-10, cultured in MDA-MB-231 for 72 hours**

Photo credit: Dr. Hazim Al-Jewari



**Figure 21: 10 uM ZIF-9, cultured in MDA-MB-231 for 48 hours**